# Imaginary potential and thermal width in the spinning black hole background from holography

Zhou-Run Zhu,[1,*] Sheng Wang,[2,†] Yang-Kang Liu,[2,‡] and Defu Hou[2,§]

[1]*School of Physics and Telecommunications Engineering, Zhoukou Normal University, Zhoukou 466001, China*

[2]*Institute of Particle Physics and Key Laboratory of Quark and Lepton Physics (MOS), Central China Normal University, Wuhan 430079, China*

(Received 7 April 2025; accepted 5 June 2025; published 7 July 2025)

In this study, we investigate the imaginary potential of heavy quarkonium in the spinning black hole background. Then, we estimate the thermal width, which is determined by the imaginary part of the finite-temperature potential. In the ultralocal description, the boosted fluid represents a globally rotating fluid. Using a holographic approach, we systematically analyze how the boost parameter influences these quantities. Our results reveal that increasing the boost parameter causes the imaginary potential to emerge at smaller interquark distances, suggesting that the boost parameter accelerates quarkonium melting. Furthermore, we find that the boost parameter enhances the thermal width, indicating greater instability of the bound state at higher boost parameter values. Notably, we observe that the effect of the boost parameter on quarkonium dissociation is more pronounced when the axis of the quark-antiquark pair is transverse to the direction of the boost parameter.

DOI: 10.1103/rwrh-z742

## I. INTRODUCTION

Heavy quarkonium consists of a heavy quark and a heavy antiquark, serving as a powerful probe for understanding the properties of quark-gluon plasma (QGP). The melting of heavy quarkonium is one of the primary experimental indications of the formation of QGP. One piece of direct evidence of this is the suppression of heavy quarkonium due to color screening [1]. Another reason for the suppression is the imaginary part of the potential. Some related studies [2–4] suggested that the imaginary potential may play a more critical role in explaining the thermal properties of quarkonium within a strongly coupled medium. The imaginary potential can explain the dissociation and decay of the bound state. Additionally, it can be used to estimate the thermal width of quarkonium related to thermal decay [5–7].

The noncentral heavy-ion collisions experiments have shown the generation of nonzero angular momentum [8–12]. While part of the angular momentum is carried away by spectator partons, a significant portion is transferred to the strongly coupled plasma [13,14]. In [11], the results from the Star Collaboration on the $\Lambda$ and $\Lambda^-$ baryons provide strong evidence and yield an angular velocity average value $\omega \sim 6$ MeV. The prediction of heavy-ion collision hydrodynamic simulations [12] suggests that the magnitude of the angular velocity can be larger, $\omega \sim (20\text{–}40)$ MeV. These nonzero angular velocity values result in relativistic rotation of the strongly coupled plasma. Investigating the influence of rotation on the thermodynamics of heavy quarkonium is an attractive research topic.

The AdS/CFT correspondence [15–17] serves as a powerful nonperturbative method for investigating the properties of strongly coupled systems and offers valuable insights into the behavior of heavy quarks in strongly coupled plasma. In the context of holography, quarks correspond to the end points of open strings that are embedded in the bulk of anti–de Sitter (AdS) spacetime. A quark-antiquark pair is represented by a string that connects the two end points. This string forms on a U-shaped configuration and its dynamics are described by the Nambu-Goto action. By using the AdS/CFT correspondence, Noronha and Dumitru first calculated the imaginary potential in $\mathcal{N} = 4$ super-Yang-Mills theory from thermal fluctuations [18]. The study of the imaginary potential of heavy quarkonium has gained significant attention. The authors of Ref. [19] discussed the imaginary potential and calculated the thermal width from an

*Contact author: zhuzhourun@zknu.edu.cn
†Contact author: shengwang@mails.ccnu.edu.cn
‡Contact author: ykl@mails.ccnu.edu.cn
§Contact author: houdf@mail.ccnu.edu.cn

imaginary potential in the static background. The dissociation of heavy quarkonium in the moving case was studied in [20]. The usual method is to boost the particle pair into a reference frame where they appear at rest, while the hot wind moves toward them. Additionally, the imaginary potential in the moving cases was studied in [21,22]. In Refs. [23,24], the authors investigated the influence of finite 't Hooft coupling corrections on the imaginary potential and the thermal width. The imaginary potential and the thermal width within AdS/QCD can be seen in [25–27]. The imaginary potential in the rotating matter was studied in [28]. In Ref. [29], the authors explored the imaginary potential in the anisotropic plasma. Other related works can be seen in [30–35].

In this work, we want to explore the imaginary potential and estimate the thermal width from the imaginary potential in the spinning black hole background from holography. It should be mentioned that the authors of Ref. [28] extended the static black hole to a local rotating background by the Lorentz transformation [36–38], and calculated the imaginary potential in the rotating background. From this Lorentz transformation, the resulting black hole is a (hyper)cylindrical surface about the symmetry axis and just represents a small area around the rotating radius $L$ with a domain range less than $2\pi$. Additionally, the string breaking and running coupling behavior of heavy quark-antiquark pairs were systematically investigated in a rotating background [39]. Furthermore, Refs. [40–42] explored heavy-quark dynamics in a rotating quark-gluon plasma, with particular focus on the drag force and jet quenching parameter in the rotational background.

It is meaningful to examine the imaginary potential and estimate the thermal width from the imaginary potential in the spinning black hole background from holography [43–47]. As discussed in [46], Myers-Perry black holes (spinning black holes) are the solutions in higher-dimensional spacetimes under Einstein gravity, which describe a rotating black hole with independent angular momentum. The boundary of the spacetime is typically compact, which leads to a gauge theory that lives on a spacetime $S^3 \times \mathbb{R}$. In the limit of a large black hole, the Myers-Perry line element becomes a Schwarzschild black brane boosted along the $x_3$ direction. The component associated with the black hole dominates and exhibits correspondence with a rigidly rotating fluid in $S^3 \times \mathbb{R}$. When projecting this flow onto flat spacetime, one observes a fluid exhibiting markedly nontrivial vorticity and expansion. Local flow analysis reveals that at leading order in the large black hole expansion, the fluid manifests as a uniformly boosted fluid, while the next-to-leading-order correction incorporates a rotation about the boost direction [47]. When investigating rotational effects, we consider zooming in on a small patch and observe a uniformly streaming fluid. In the ultralocal description, the boosted fluid represents a globally rotating fluid. In the dual field theory, the planar black brane is particularly relevant for understanding the behavior of the QGP. Inspired by this, we aim to examine the impact of the boost parameter on the imaginary potential and estimate the thermal width from the imaginary potential in the Myers-Perry black hole background.

The paper is organized as follows. In Sec. II, we briefly review the spinning black hole background. In Sec. III, we explore the imaginary potential and estimate the thermal width from the imaginary potential in the Myers-Perry black hole background. In Sec. IV, we give the conclusion and discussion.

## II. SPINNING MYERS-PERRY BLACK HOLE BACKGROUND

In this work, we aim to investigate the imaginary potential and estimate the thermal width from the imaginary potential in the Myers-Perry black hole background. We first briefly review the metric of a five-dimensional spinning black hole background, which was proposed by Hawking *et al.* [43],

$$\begin{aligned} ds^2 =& -\frac{\Delta}{\rho^2}\left(dt_H - \frac{a\sin^2\theta_H}{\Xi_a}d\phi_H - \frac{b\cos^2\theta_H}{\Xi_b}d\psi_H\right)^2 \\ &+ \frac{\Delta_{\theta_H}\sin^2\theta_H}{\rho^2}\left(adt_H - \frac{r_H^2+a^2}{\Xi_a}d\phi_H\right)^2 \\ &+ \frac{\Delta_{\theta_H}\cos^2\theta_H}{\rho^2}\left(bdt_H - \frac{r_H^2+b^2}{\Xi_b}d\psi_H\right)^2 + \frac{\rho^2}{\Delta}dr_H^2 \\ &- \frac{\rho^2}{\Delta_{\theta_H}}d\theta_H^2 + \frac{1+\frac{r_H^2}{L^2}}{r_H^2\rho^2}\left(abdt_H - \frac{b(r^2+a^2)\sin^2\theta_H}{\Xi_a}d\phi_H \right. \\ &\left. - \frac{a(r^2+b^2)\cos^2\theta_H}{\Xi_b}d\psi_H\right)^2, \end{aligned} \tag{1}$$

with

$$\begin{aligned} \Delta &= \frac{1}{r_H^2}(r_H^2+a^2)(r_H^2+b^2)\left(1+\frac{r_H^2}{L^2}\right) - 2M, \\ \Delta_{\theta_H} &= 1 - \frac{a^2}{L^2}\cos^2\theta_H - \frac{b^2}{L^2}\sin^2\theta_H, \\ \rho &= r_H^2 + a^2\cos^2\theta_H + b^2\sin^2\theta_H, \\ \Xi_a &= 1 - \frac{a^2}{L^2}, \\ \Xi_b &= 1 - \frac{b^2}{L^2}, \end{aligned} \tag{2}$$

where $a$ and $b$ are the angular momentum parameters. In this work, we consider the spinning Myers-Perry black hole case, namely, the $a = b$ case [44,45]. In addition, $\phi_H$, $\psi_H$, and $\theta_H$ represent angular Hopf coordinates. $t_H$ denotes time, $L$ is the AdS radius, and $r_H$ represents the AdS radial coordinate. $M$ is the mass.

After adopting the more convenient coordinates [48]

$$\begin{aligned} t &= t_H, \\ r^2 &= \frac{a^2 + r_H^2}{1 - \frac{a^2}{L^2}}, \\ \theta &= 2\theta_H, \\ \phi &= \phi_H - \psi_H, \\ \psi &= -\frac{2at_H}{L^2} + \phi_H + \psi_H, \\ b &= a, \\ \mu &= \frac{M}{(L^2 - a^2)^3}, \end{aligned} \tag{3}$$

one can rewrite the metric (1) as

$$\begin{aligned} ds^2 = &-\left(1 + \frac{r^2}{L^2}\right)dt^2 + \frac{dt^2}{G(\mathrm{r})} + \frac{r^2}{4}\left((\sigma^1)^2 + (\sigma^2)^2 + (\sigma^3)^2\right) \\ &+ \frac{2\mu}{r^2}\left(dt + \frac{a}{2}\sigma^3\right)^2, \end{aligned} \tag{4}$$

with

$$\begin{aligned} G(r) &= 1 + \frac{r^2}{L^2} - \frac{2\mu\left(1 - \frac{a^2}{L^2}\right)}{r^2} + \frac{2\mu a^2}{r^4}, \\ \mu &= \frac{r_h^4(L^2 + r_h^2)}{2L^2 r_h^2 - 2a^2(L^2 + r_h^2)}, \\ \sigma^1 &= -\sin\psi dt d\theta + \cos\psi \sin\theta d\phi, \\ \sigma^2 &= \cos\psi d\theta + \sin\psi \sin\theta d\phi, \\ \sigma^3 &= d\psi + \cos\theta d\phi, \end{aligned} \tag{5}$$

where

$$\begin{aligned} -\infty < t < \infty, \qquad r_h < r < \infty, \qquad 0 \le \theta \le \pi, \\ 0 \le \phi \le 2\pi, \qquad 0 \le \psi \le 4\pi. \end{aligned} \tag{6}$$

The planar black brane can be obtained by the coordinate transformation [46]

$$\begin{aligned} t &= \tau, \\ \frac{L}{2}(\phi - \pi) &= x_1, \\ \frac{L}{2}\tan\left(\theta - \frac{\pi}{2}\right) &= x_2, \\ \frac{L}{2}(\psi - 2\pi) &= x_3, \\ r &= \tilde{r}, \end{aligned} \tag{7}$$

where $(\tau, \tilde{r}, x_1, x_2, x_3)$ denote new coordinates. These coordinates can be scaled with a factor $\beta$,

$$\begin{aligned} \tau &\to \beta^{-1}\tau, \\ x_1 &\to \beta^{-1}x_1, \\ x_2 &\to \beta^{-1}x_2, \\ x_3 &\to \beta^{-1}x_3, \\ \tilde{r} &\to \beta\tilde{r}, \\ \tilde{r_h} &\to \beta\tilde{r_h}(\beta \to \infty). \end{aligned} \tag{8}$$

One can derive the metric of a Schwarzschild black brane, which is boosted in the $\tau$-$x_3$ plane [46],

$$\begin{aligned} ds^2 = \frac{r^2}{L^2}\Bigg(&-d\tau^2 + dx_1^2 + dx_2^2 + dx_3^2 \\ &+ \frac{r_h^4}{r^4\left(1 - \frac{a^2}{L^2}\right)}\left(d\tau + \frac{a}{L}dx_3\right)^2\Bigg) + \frac{L^2 r^2}{r^4 - r_h^4}dr^2, \end{aligned} \tag{9}$$

where the Schwarzschild black brane can be recovered when the boost parameter vanishes ($a = 0$).

Then, we take $z$ ($r = 1/z$) as the holographic fifth coordinate for simplified calculations,

$$\begin{aligned} ds^2 = \frac{1}{z^2 L^2}\Bigg[&-d\tau^2 + dx_1^2 + dx_2^2 + dx_3^2 \\ &+ \frac{z^4}{z_h^4\left(1 - \frac{a^2}{L^2}\right)}\left(d\tau + \frac{a}{L}dx_3\right)^2\Bigg] + \frac{L^2 z_h^4}{z^2\left(z_h^4 - z^4\right)}dz^2. \end{aligned} \tag{10}$$

The expression for the temperature is [46]

$$T_h = \frac{\sqrt{L^2 - a^2}}{z_h \pi L^3}, \tag{11}$$

where $z_h$ denotes the horizon. In the limit of a large black hole, the angular velocity $\Omega = a/L^2$ [46]. In the following calculations, we take the AdS radius $L = 1$ for simplicity.

## III. IMAGINARY POTENTIAL AND THERMAL WIDTH IN SPINNING MYERS-PERRY BLACK HOLE BACKGROUND

In this section, we explore the imaginary potential and estimate the thermal width from the imaginary potential in the spinning background, which could be calculated from the on-shell action of the world sheet. The formulas can be derived by following the steps in Refs. [18,19,29].

The on-shell Nambu-Goto (NG) action is

$$S = -\frac{1}{2\pi\alpha'}\int d\tau d\sigma \sqrt{-\det g_{\alpha\beta}}, \tag{12}$$

where $g_{\alpha\beta}$ is the determinant of the induced metric. $\tau$ and $\sigma$ represent the world-sheet coordinates.

In the following discussion, we explore the impact of the boost parameter in different directions. The gravitational metric can be viewed as boosted in the $\tau$-$x_3$ plane, indicating that the direction of rotation is along the $x_3$ direction. Meanwhile, the axis of the $Q\bar{Q}$ pair in the $x_1$-$x_2$ plane is considered a transverse case, whereas the axis of the $Q\bar{Q}$ pair aligned with $x_3$ is regarded as a parallel case.

In the transverse case, the world-sheet coordinates can be parametrized by

$$\tau = \xi, \qquad x_1 = \eta, \qquad x_2 = 0, \qquad x_3 = 0, \qquad z = z(\eta). \tag{13}$$

The Lagrangian density can be obtained as

$$\mathcal{L} = \sqrt{A(z) + B(z)\dot{z}^2}, \tag{14}$$

with

$$A(z) = A(z_\perp) = \frac{1}{z^4} - \frac{1}{z_h^4(1-a^2)},$$
$$B(z) = B(z_\perp) = \frac{z_h^4}{z^4\left(z_h^4 - z^4\right)} - \frac{1}{\left(z_h^4 - z^4\right)(1-a^2)}. \tag{15}$$

In the parallel case, the world-sheet coordinates can be parametrized by

$$\tau = \xi, \qquad x_1 = 0, \qquad x_2 = 0, \qquad x_3 = \eta, \qquad z = z(\eta). \tag{16}$$

The expressions for $A(z)$ and $B(z)$ are

$$A(z) = A(z_\parallel) = \frac{z_h^4 - z^4}{z^4 z_h^4},$$
$$B(z) = B(z_\parallel) = \frac{z_h^4}{z^4\left(z_h^4 - z^4\right)} - \frac{1}{\left(z_h^4 - z^4\right)(1-a^2)}. \tag{17}$$

The interquark distance $L$ of $Q\bar{Q}$ is

$$L = 2\int_0^{z_*} \sqrt{\frac{A(z_*)B(z)}{A(z)^2 - A(z)A(z_*)}}dz, \tag{18}$$

where $z_*$ $(0 < z_* < z_h)$ is the deepest point of the U-shaped string.

The imaginary potential can be calculated from the thermal fluctuations of the string world sheet [18]. One can incorporate thermal fluctuations $\delta z(x)$ about the classical world-sheet configuration $z_c(x)$, where $\delta z(x)$ characterizes thermal excitations of the string,

$$z(x) = z_c(x) \to z(x) = z_c(x) + \delta z(x). \tag{19}$$

In the long-wavelength fluctuations approximation for string fluctuations, where the string end point $z_*$ is sufficiently close to the horizon $z_h$, certain fluctuation modes can penetrate the horizon region. The partition function, including thermal fluctuation effects, then takes the form

$$Z_{\rm str} \sim \int \mathcal{D}\delta z(x) e^{iS_{\rm NG}(z_c(x)+\delta z(x))}. \tag{20}$$

We evaluate the $\delta z(x)$ integral numerically by introducing a uniform discretization of the interval $[-\frac{L}{2}, \frac{L}{2}]$ with $2N$ parts, establishing grid points at $x_j = j\Delta x = j\frac{L}{2N}$:

$$Z_{\rm str} \sim \lim_{N\to\infty} d[\delta z(x_{-N})]\cdots d[\delta z(x_N)] \times \exp\left[\frac{i\mathcal{T}\Delta x}{2\pi\alpha'}\sum_j \sqrt{A(z_j) + B(z_j)z_j'^2}\right], \tag{21}$$

where $z_j \equiv z(x_j)$, $z_j' \equiv \frac{dz(x)}{dx}|_{x=x_j}$. Since the thermal fluctuations are predominantly localized near the bottom of the string (corresponding to $x = 0$ where $z = z_*$), we can expand $z_c(x_j)$ around $x = 0$ while retaining only terms up to second order in $x_j$. This approximation is justified by the fact that $z_c'(0) = 0$ at this point,

$$z_c(x_j) \simeq z_* + \frac{x_j^2}{2}z_c''(0). \tag{22}$$

One can expand $A(z_j)$ and keep terms up to second order in $x_j^m\delta z_n$,

$$A(z_j) \approx A_* + A_*'\frac{x_j^2}{2}z_c''(0) + A_*'\delta z + A_*''\frac{\delta z^2}{2}, \tag{23}$$

where $A_* \equiv A(z_*), A(z_*) \equiv \frac{\partial A(z)}{\partial z}|_{z=z_*}$, etc. The exponent in Eq. (21) can be approximated as

$$S_j^{\rm NG} = \frac{\mathcal{T}\Delta x}{2\pi\alpha'}\sqrt{C_1 x_j^2 + C_2}, \tag{24}$$

where

$$C_1 = \frac{z_c''(0)}{2}[2B_*z_c''(0) + A_*'],$$
$$C_2 = A_* + \delta z A_*' + \frac{\delta z^2}{2}A_*''. \tag{25}$$

The analysis reveals that if $S_j^{\rm NG}$ induces an imaginary component in the potential, the argument of the square root in Eq. (24) becomes negative. For the $j$th contribution, this yields

$$I_j \equiv \int_{\delta z_{j\min}}^{\delta z_{j\max}} \exp\left[\frac{i\mathcal{T}\Delta x}{2\pi\alpha'}\sqrt{C_1 x_j^2 + C_2}\right], \tag{26}$$

where $\delta z_{j\min}$ and $\delta z_{j\max}$ denote the roots of $C_1 x_j^2 + C_2$ in $\delta z$. The integral can be evaluated via the saddle-point approximation, with the stationary point occurring when the argument of the square root in Eq. (26) satisfies the extremum condition,

$$D(z_j) \equiv C_1 x_j^2 + C_2(\delta z_j), \tag{27}$$

which happens for

$$\delta z = -\frac{A'_*}{A''_*}. \tag{28}$$

The condition for the square root to develop an imaginary part requires $x_j < |x_c|$,

$$x_c = \sqrt{\frac{1}{C_1}\left(\frac{A'_*}{2A''_*} - A_*\right)}. \tag{29}$$

The complete contribution arises from summing individual terms, yielding $\Pi_j I_j$. This gives the result

$$\mathrm{Im}\, V = -\frac{1}{2\pi\alpha'}\int_{|x|<x_c} dx\sqrt{-C_1 x^2 - A_* + \frac{A_*^2}{2A'^2_*}}. \tag{30}$$

Integrating Eq. (30) yields the expression for the imaginary potential $\mathrm{Im}\, V$,

$$\mathrm{Im}\, V = -\frac{\sqrt{\lambda}}{2\sqrt{2}}\sqrt{B(z_*)}\left(\frac{A'(z_*)}{2A''(z_*)} - \frac{A(z_*)}{A'(z_*)}\right), \tag{31}$$

where $A'(z_*)$ and $A''(z_*)$ are the first and second derivative of $A(z_*)$, respectively.

To obtain the thermal width, one could derive the expectation value of the imaginary potential using the nonrelativistic approximation [18,19]

$$\Gamma = -\langle\psi|\,\mathrm{Im}\, V|\psi\rangle, \tag{32}$$

where

$$\langle\vec{r}|\psi\rangle = \frac{1}{\sqrt{\pi}a_0^{3/2}}e^{-r/a_0} \tag{33}$$

is the ground-state wave function of a particle and the particle has a Coulomb-like potential. Thus, one can obtain the thermal width $\Gamma$ defined by the imaginary potential.

The thermal width of $Q\bar{Q}$ is

$$\Gamma/T = -\frac{4}{(a_0 T)^3}\int d\omega\omega^2 e^{\frac{-2\omega}{a_0 T}}\frac{ImV(\omega)}{T}, \tag{34}$$

where $\omega = LT$ and $a_0$ is the Bohr radius. There is an exact approach and an approximate approach to calculate the thermal width [19,29]. It should be mentioned that the authors of [32] studied the effect of gluon condensate on the thermal width by the exact and approximate approaches. The qualitative results from the two approaches are consistent. In this work, we adopt the approximate approach to discuss the effect of the boost parameter on the thermal width.

We examine the imaginary potential and estimate the thermal width from the imaginary potential in the spinning Myers-Perry black hole from Eqs. (18), (31), and (34). For our calculations, we take $\lambda = 1$. According to Ref. [46], the background geometry features a planar black brane at high temperatures. Therefore, we choose a high temperature $T = 100/\pi$. Additionally, the background remains stable when $a < 0.75L$. Thus, we take $a = 0.1, 0.2, 0.3$ in the numerical calculations. It should be mentioned that the spinning background is dual to the rotating QGP system. The behavior of QGP flow can be visualized as a uniform motion, characterized by uniformly rotating circles of a Hopf fibration within the spatial component of four-dimensional spacetime [47].

Then, we discuss three restrictions on the imaginary potential. First, the term $B(z_*)$ in Eq. (31) must be positive. Second, the imaginary potential should be negative. This requirement implies that $(\frac{A'(z_*)}{2A''(z_*)} - \frac{A(z_*)}{A'(z_*)}) > 0$ in Eq. (31), leading to the condition $\varepsilon > \varepsilon_{\min}$ ($\varepsilon \equiv z_*/z_h$). The last restriction is related to the maximum value of $LT$, denoted as $LT_{\max}$. In Fig. 1(a), we draw the interquark distance $LT$ versus $\varepsilon$ with different values of the boost parameter $a$. It can be observed that $LT$ increases monotonically with $\varepsilon$ and reaches a maximum value, $LT_{\max}$, at $\varepsilon = \varepsilon_{\max}$. This feature suggests that the string is a U-shape type. When $\varepsilon > \varepsilon_{\max}$, $LT$ decreases monotonically with $\varepsilon$, indicating that the string configurations solutions no longer satisfy the NG action [49]. Therefore, we restrict our calculations to the range $\varepsilon_{\min} < \varepsilon < \varepsilon_{\max}$ ($LT_{\min} < LT < LT_{\max}$) in the calculations. We also find that the presence of the boost parameter suppresses $LT_{\max}$, suggesting that the boost parameter favors the dissociation of quarkonium. Moreover, the dissociation effect is stronger in the transverse cases.

In Fig. 1(b), we depict the imaginary potential $\mathrm{Im}\, V/(\sqrt{\lambda}T)$ of quarkonium as a function of $LT$ with a different boost parameter $a$. The imaginary potential begins at $LT_{\min}$ and ends at $LT_{\max}$. It is evident that the imaginary potential appears at smaller $LT$ as the boost parameter increases. As noted in Ref. [21], the suppression becomes

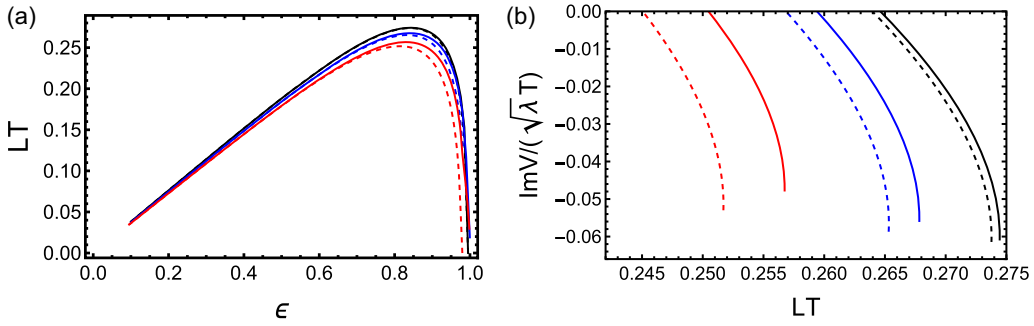


FIG. 1. (a) $LT$ versus $\epsilon$ with different boost parameter $a$. (b) Imaginary potential $\mathrm{Im}\, V/(\sqrt{\lambda}T)$ of quarkonium versus $LT$ with different boost parameter $a$. In panel (a) from top to bottom $a = 0.1$, 0.2, 0.3, respectively. In panel (b) from right to left $a = 0.1$, 0.2, 0.3, respectively. The solid line (dashed line) represents the parallel (transverse) case.

stronger when the imaginary potential occurs at smaller $LT$. Therefore, we can conclude that the boost parameter contributes to the melting of quarkonium. Additionally, the impact of the boost parameter on the imaginary potential is more significant in the transverse case compared with the parallel case.

The authors of Ref. [28] extended the static black hole to a local rotating background by the Lorentz transformation and calculated the imaginary potential in this local rotating background. They found that the angular momentum enhances the dissociation. Although the rotating backgrounds considered are different, our results coincide with the results of Ref. [28].

Next, we examine how the boost parameter affects the thermal width. We plot the thermal width $\Gamma/T$ against $a_0T$ for various values of the boost parameter $a$ in Fig. 2. One can observe that the boost parameter enhances the thermal width, with a more significant effect observed in the transverse case than in the parallel case. A larger thermal width indicates that the state is unstable and may break down into free quarks, whereas a smaller thermal width suggests a more stable bound state. This phenomenon can be explained by the binding energy of heavy quarkonium. The authors of Ref. [50] investigated the thermodynamics of heavy quarkonium in the spinning black hole background and calculated its binding energy. They discovered that the binding energy increases quickly to zero when increasing the boost parameter, indicating that heavy quarkonium is more unstable at larger values of the boost parameter. The authors of Ref. [51] examined the spectral function of heavy quarkonium within the same spinning black hole background and found that the boost parameter facilitates the dissociation of heavy quarkonium. Our results are consistent with those presented in Refs. [50,51].

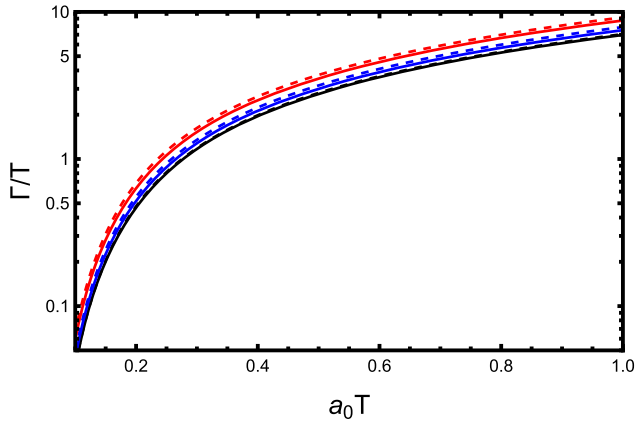


FIG. 2. Thermal width $\Gamma/T$ versus $a_0T$ with different boost parameter $a$. From bottom to top $a = 0.1$, 0.2, 0.3, respectively. The solid line (dashed line) represents the parallel (transverse) case.

## IV. CONCLUSION AND DISCUSSION

In this paper, we investigated the imaginary potential and estimated the thermal width from the imaginary potential in the spinning black hole background. The imaginary potential could explain the dissociation and decay of the bound state. Also, it can be used to estimate the thermal width related to thermal decay.

We found that the boost parameter suppresses the maximum value of the interquark distance $LT$. As the boost parameter increases, the imaginary potential appears at smaller $LT$, indicating that the boost parameter contributes to the melting of quarkonium. Additionally, we observed that the boost parameter enhances the thermal width, indicating that the bound state is more unstable at larger values of the boost parameter. Furthermore, we concluded that the boost parameter has a stronger effect on the dissociation of quarkonium when the axis of the quark-antiquark pair $Q\bar{Q}$ is transverse to the direction of the boost parameter.

The study of the imaginary potential and the calculation of the thermal width from the imaginary potential under rotation is crucial for understanding their behavior in rotating thermal QGP, which contributes to investigating the quarkonium suppression and thermalization in heavy-ion collisions experiments. Finally, investigating the configuration entropy within a spinning black hole may be a meaningful work. We plan to delve into this topic in our subsequent studies.

## ACKNOWLEDGMENTS

D. H.'s research is supported in part by the National Key Research and Development Program of China under Contract No. 2022YFA1604900. Additionally, he receives partial support from the National Natural Science Foundation of China under Grants No. 12435009, and No. 12275104. Z.-R. Z. is supported by the startup Foundation projects for Doctors at Zhoukou Normal University, with the Project No. ZKNUC2023018. Z.-R. Z. is also supported by the Natural Science Foundation of Henan Province of China under Grant No. 242300420947.

## DATA AVAILABILITY

The data are not publicly available. The data are available from the authors upon reasonable request.

[1] T. Matsui and H. Satz, Phys. Lett. B **178**, 416 (1986).
[2] M. Laine, O. Philipsen, P. Romatschke, and M. Tassler, J. High Energy Phys. 03 (2007) 054.
[3] A. Beraudo, J. P. Blaizot, and C. Ratti, Nucl. Phys. **A806**, 312 (2008).
[4] Y. Burnier, M. Laine, and M. Vepsalainen, Phys. Lett. B **678**, 86 (2009).
[5] N. Brambilla, M. A. Escobedo, J. Ghiglieri, J. Soto, and A. Vairo, J. High Energy Phys. 09 (2010) 038.
[6] N. Brambilla, J. Ghiglieri, A. Vairo, and P. Petreczky, Phys. Rev. D **78**, 014017 (2008).
[7] M. Margotta, K. McCarty, C. McGahan, M. Strickland, and D. Yager-Elorriaga, Phys. Rev. D **83**, 105019 (2011); **84**, 069902(E) (2011).
[8] Z. T. Liang and X. N. Wang, Phys. Rev. Lett. **94**, 102301 (2005); **96**, 039901(E) (2006).
[9] F. Becattini, F. Piccinini, and J. Rizzo, Phys. Rev. C **77**, 024906 (2008).
[10] M. Baznat, K. Gudima, A. Sorin, and O. Teryaev, Phys. Rev. C **88**, 061901 (2013).
[11] STAR Collaboration, Nature (London) **548**, 62 (2017).
[12] Y. Jiang, Z. W. Lin, and J. Liao, Phys. Rev. C **94**, 044910 (2016); **95**, 049904(E) (2017).
[13] M. I. Baznat, K. K. Gudima, A. S. Sorin, and O. V. Teryaev, Phys. Rev. C **93**, 031902 (2016).
[14] D. E. Kharzeev, J. Liao, S. A. Voloshin, and G. Wang, Prog. Part. Nucl. Phys. **88**, 1 (2016).
[15] J. M. Maldacena, Adv. Theor. Math. Phys. **2**, 231 (1998).
[16] E. Witten, Adv. Theor. Math. Phys. **2**, 253 (1998).
[17] S. S. Gubser, I. R. Klebanov, and A. M. Polyakov, Phys. Lett. B **428**, 105 (1998).
[18] J. Noronha and A. Dumitru, Phys. Rev. Lett. **103**, 152304 (2009).
[19] S. I. Finazzo and J. Noronha, J. High Energy Phys. 11 (2013) 042.
[20] H. Liu, K. Rajagopal, and U. A. Wiedemann, Phys. Rev. Lett. **98**, 182301 (2007).
[21] S. I. Finazzo and J. Noronha, J. High Energy Phys. 01 (2015) 051.
[22] M. Ali-Akbari, D. Giataganas, and Z. Rezaei, Phys. Rev. D **90**, 086001 (2014).
[23] K. B. Fadafan and S. K. Tabatabaei, Eur. Phys. J. C **74**, 2842 (2014).
[24] K. Bitaghsir Fadafan and S. K. Tabatabaei, J. Phys. G **43**, 095001 (2016).
[25] J. Sadeghi and S. Tahery, J. High Energy Phys. 06 (2015) 204.
[26] N. R. F. Braga and L. F. Ferreira, Phys. Rev. D **94**, 094019 (2016).
[27] Z. q. Zhang and X. Zhu, Phys. Lett. B **793**, 200 (2019).
[28] Z. q. Zhang, X. Zhu, and D. f. Hou, Nucl. Phys. **B989**, 116149 (2023).
[29] K. Bitaghsir Fadafan, D. Giataganas, and H. Soltanpanahi, J. High Energy Phys. 11 (2013) 107.
[30] Z. q. Zhang, D. f. Hou, and G. Chen, Phys. Lett. B **768**, 180 (2017).
[31] Z. q. Zhang and D. f. Hou, Phys. Lett. B **778**, 227 (2018).
[32] Y. Q. Zhao, Z. R. Zhu, and X. Chen, Eur. Phys. J. A **56**, 57 (2020).
[33] M. Kioumarsipour and J. Sadeghi, Eur. Phys. J. C **81**, 735 (2021).
[34] M. Kioumarsipour and B. Khanpour, Phys. Lett. B **855**, 138791 (2024).
[35] J. L. Albacete, Y. V. Kovchegov, and A. Taliotis, Phys. Rev. D **78**, 115007 (2008).
[36] C. Erices and C. Martinez, Phys. Rev. D **97**, 024034 (2018).
[37] M. Bravo Gaete, L. Guajardo, and M. Hassaine, J. High Energy Phys. 04 (2017) 092.
[38] A. M. Awad, Classical Quantum Gravity **20**, 2827 (2003).
[39] J. Zhou, S. Zhang, J. Chen, L. Zhang, and X. Chen, Phys. Lett. B **844**, 138116 (2023).
[40] I. Y. Aref'eva, A. A. Golubtsova, and E. Gourgoulhon, J. High Energy Phys. 04 (2021) 169.
[41] A. A. Golubtsova, E. Gourgoulhon, and M. K. Usova, Nucl. Phys. **B979**, 115786 (2022).
[42] I. Aref'eva, A. Golubtsova, and E. Gourgoulhon, Phys. Part. Nucl. **51**, 535 (2020).
[43] S. W. Hawking, C. J. Hunter, and M. Taylor, Phys. Rev. D **59**, 064005 (1999).
[44] G. W. Gibbons, M. J. Perry, and C. N. Pope, Classical Quantum Gravity **22**, 1503 (2005).

[45] G. W. Gibbons, H. Lu, D. N. Page, and C. N. Pope, Phys. Rev. Lett. **93**, 171102 (2004).
[46] M. Garbiso and M. Kaminski, J. High Energy Phys. 12 (2020) 112.
[47] M. A. G. Amano, C. Cartwright, M. Kaminski, and J. Wu, Prog. Part. Nucl. Phys. **139**, 104135 (2024).
[48] K. Murata, Prog. Theor. Phys. **121**, 1099 (2009).
[49] D. Bak, A. Karch, and L. G. Yaffe, J. High Energy Phys. 08 (2007) 049.
[50] Z. R. Zhu, S. Wang, X. Chen, J. X. Chen, and D. Hou, Phys. Rev. D **110**, 126008 (2024).
[51] Z. R. Zhu, M. Sun, R. Zhou, Z. Ma, and J. Han, Eur. Phys. J. C **84**, 1252 (2024).